Outage Performance of Integrated Satellite-Terrestrial Networks With Hybrid CCI

Yuhan Ruan, Yongzhao Li, Cheng-Xiang Wang, *Fellow, IEEE*, Rui Zhang, and Hailin Zhang

***Abstract*— We investigate the outage performance of an integrated satellite-terrestrial network undergoing hybrid co-channel interference (CCI), which comprises inter-component CCI from the satellite and intra-component CCI from adjacent base stations. Taking the interference power constraints imposed by satellite communications into account, we derive a closed-form expression for the outage probability (OP) of the terrestrial network, where the satellite link and terrestrial links are modeled as shadowed-Rician and Nakagami-m fading, respectively. Finally, simulation results demonstrate the validity of the theoretical analysis and show the effects of various key parameters on the OP performance.**

***Index Terms*— Integrated satellite-terrestrial networks, hybrid co-channel interference, interference power constraints, outage probability.**

I. Introduction

HAVING the ability to provide ubiquitous coverage and spatially optimize the usage of scarce spectrum resource, the integrated satellite-terrestrial network is becoming an attractive and promising infrastructure for future multimedia services [1]. In the integrated network, the terrestrial component is complementary to the satellite component and licensed to operate in the same frequency band as the satellite segment [2]. Although the frequency reuse between satellite and terrestrial components can improve the spectral efficiency of the overall system, it will inevitably cause co-channel interference (CCI), which is the major challenge of the integrated network. In this regard, the authors in [3] presented several interference scenarios while a position based interference mitigation scheme was proposed in [4]. Moreover, the authors in [5] investigated the symbol error rate performance of a satellite-terrestrial cooperative network with CCI at the destination.

The above work mainly studied the inter-component CCI between satellite and terrestrial communications. However, in the integrated network, when cellular users are located at the cell edge overlapped by both the satellite and the terrestrial components, they would also suffer from the intra-component CCI from adjacent base stations (BSs), resulting in hybrid CCI together with the inter-component CCI from the satellite. Among the existing studies, the authors in [6] investigated the impacts of hybrid CCI on the integrated network, while the spatial distribution of the interfering BSs and interference management were not considered. To fill this gap, this letter extends the scenario in [6] to a more general one, where the interfering BSs are characterized as points of a Poisson point process (PPP) [7]. Under this situation, we investigate the outage performance for an integrated satellite-terrestrial network undergoing hybrid CCI. A closed-form expression for the outage probability (OP) of the terrestrial network is derived while satisfying the interference power constraints imposed by satellite communications.

Manuscript received February 24, 2017; accepted April 5, 2017. Date of publication April 12, 2017; date of current version July 8, 2017. The associate editor coordinating the review of this paper and approving it for publication was L. Mucchi. The authors gratefully acknowledge the support from the EU H2020 RISE TESTBED project (No. 734325), EU FP7 QUICK project (No. PIRSES-GA-2013-612652), EPSRC TOUCAN project (No. EP/L020009/1), the 111project (B08038), and the National Key Research and Development Program of China (2016YF-B1200202) *(Corresponding author: Yongzhao Li.)*

Y. Ruan, Y. Li, R. Zhang, and H. Zhang are with the State Key Laboratory of Integrated Services Networks, Xidian University, Xi'an 710071, China (e-mail: ryh911228@163.com; yzhli@xidian.edu.cn; rui.zhang@stu.xidian.edu.cn; hlzhang@xidian.edu.cn).

C.-X. Wang is with the Institute of Sensors, Signals and Systems, School of Engineering and Physical Sciences, Heriot-Watt University, Edinburgh EH14 4AS, U.K. (e-mail: cheng-xiang.wang@hw.ac.uk).

Digital Object Identifier 10.1109/LCOMM.2017.2694005

II. System Model

We focus on the cellular users located at the cell edge suffering from the inter-component CCI from the satellite and intra-component CCI from adjacent BS$_i$ ($i = 1, \cdots, N$). Considering a realistic scenario, we characterize the spatial distribution of interfering BSs as a PPP with intensity λ. Herein, N BSs are located in a finite circular area centered around the destination (D) user with radius R, beyond which the interference is assumed to be negligible due to path loss. We denote h_{bd}, $h_{i\mathrm{d}}$, h_{bf}, and h_{sd} as the channel coefficients of serving BS$\rightarrow$D, adjacent BS$_i\rightarrow$D, serving BS$\rightarrow$fixed satellite receiver, and satellite$\rightarrow$D links, respectively.

In the considered network, the received signal-to-interference-plus-noise ratio (SINR) at D can be expressed as

$$\gamma = \frac{P_{\mathrm{b}}|h_{\mathrm{bd}}|^2}{I_{\mathrm{a}} + I_{\mathrm{s}} + N_0} \tag{1}$$

where P_{b} is the transmit power of the serving BS. In the integrated network, to prevent the sensitive satellite receiver from being interfered beyond an interference power threshold I_{th} [8], P_{b} should satisfy $P_{\mathrm{b}} = \min\left(\frac{I_{\mathrm{th}}}{|h_{\mathrm{bf}}|^2}, P_{\mathrm{m}}\right)$, where P_{m} denotes the maximum transmit power of the serving BS. In (1), $I_{\mathrm{s}} = P_{\mathrm{s}}|h_{\mathrm{sd}}|^2$ is the interference power from the satellite with transmit power P_{s}, N_0 is the average noise power, and $I_{\mathrm{a}} = \sum_{i=1}^{N} P_{\mathrm{t}}|h_{i\mathrm{d}}|^2$ is the aggregate interference power received from terrestrial interferers with P_{t} as the transmit power of adjacent BS$_i$. We assume the power gain between BS$_i$ and D, $|h_{i\mathrm{d}}|^2$, decays exponentially with parameter α and follows Gamma distributions with a shape parameter k_{td} and a scale parameter η_{td}. According to [9], the aggregate interference from the PPP based BSs can be approximated as a Gamma distribution with a shape parameter $k_{\mathrm{a}} = \frac{(\mathrm{E}[I_{\mathrm{a}}])^2}{\mathrm{Var}[I_{\mathrm{a}}]}$ and a scale parameter $\eta_{\mathrm{a}} = \frac{\mathrm{Var}[I_{\mathrm{a}}]}{\mathrm{E}[I_{\mathrm{a}}]}$, i.e., $I_{\mathrm{a}} \sim \mathcal{G}(\mathrm{k_a}, \eta_{\mathrm{a}})$, where

$$\mathrm{E}[I_{\mathrm{a}}] = 2\pi P_{\mathrm{t}}\lambda\sqrt{\frac{k_{\mathrm{td}}+1}{2k_{\mathrm{td}}}}\frac{R^{2-\alpha}}{2-\alpha} \tag{2}$$

$$\mathrm{Var}[I_{\mathrm{a}}] = \pi P_{\mathrm{t}}^2\lambda k_{\mathrm{td}}(1+k_{\mathrm{td}})\eta_{\mathrm{td}}^2\frac{R^{2-2\alpha}}{1-\alpha}. \tag{3}$$

Based on the interference model and interference power limitation described above, the SINR in (1) can be rewritten as

$$\gamma = \frac{\bar{\gamma}_{\rm b}|h_{\rm bd}|^2}{\tilde{I}_{\rm a}+\tilde{I}_{\rm s}+1} \tag{4}$$

where $\bar{\gamma}_{\rm b} = P_{\rm b}/N_0 = \min\left(\bar{\gamma}_{\rm th}/|h_{\rm bf}|^2, \bar{\gamma}_{\rm m}\right)$ denotes the average signal-to-noise ratio (SNR) with $\bar{\gamma}_{\rm th} = I_{\rm th}/N_0$ and $\bar{\gamma}_{\rm m} = P_{\rm m}/N_0$. Here, we have $\tilde{I}_{\rm a} = \sum_{i=1}^{N} \bar{\gamma}_{\rm t}\,|h_{i\rm d}|^2$ with $\bar{\gamma}_{\rm t} = P_{\rm t}/N_0$, and $\tilde{I}_{\rm s} = \bar{\gamma}_{\rm s}|h_{\rm sd}|^2$ with $\bar{\gamma}_{\rm s} = P_{\rm s}/N_0$.

In the following, we provide the related channel models: The channel power gains of the terrestrial Nakagami-m fading links h_Δ ($\Delta = {\rm bd}, i{\rm d}, {\rm bf}$) follow the Gamma distribution $\mathcal{G}(k_\Delta, \eta_\Delta)$, of which the probability density function (PDF) can be expressed as

$$f_{|h_\Delta|^2}(x) = \frac{x^{k_\Delta-1}e^{-\frac{x}{\eta_\Delta}}}{\Gamma(k_\Delta)\,\eta_\Delta^{k_\Delta}} \tag{5}$$

where $\Gamma(\cdot)$ denotes the Gamma function. Meanwhile, we model the satellite link $h_{\rm sd}$ as a shadowed-Rician fading channel, and the PDF of $|h_{\rm sd}|^2$ is given as [10]

$$f_{|h_{\rm sd}|^2}(x) = \alpha_{\rm sd}e^{-\beta_{\rm sd}x}\,{}_1F_1(m_{\rm sd};1;\delta_{\rm sd}x), \quad x>0 \tag{6}$$

where $\alpha_{\rm sd} \triangleq 0.5(2b_{\rm sd}m_{\rm sd}/(2b_{\rm sd}m_{\rm sd}+\Omega_{\rm sd}))^{m_{\rm sd}}/b_{\rm sd}$, $\beta_{\rm sd} \triangleq (0.5/b_{\rm sd})$, $\delta_{\rm sd} \triangleq 0.5\Omega_{\rm sd}/\left(2b_{\rm sd}^2m_{\rm sd}+b_{\rm sd}\Omega_{\rm sd}\right)$, $\Omega_{\rm sd}$ is the average power of line-of-sight component, $2b_{\rm sd}$ is the average power of the multipath component, $0 \le m_{\rm sd} \le \infty$ is the Nakagami parameter, and ${}_1F_1(a;b;z)$ is the confluent hypergeometric function.

III. Outage Probability Analysis

We investigate the outage performance of the integrated satellite-terrestrial network suffering from inter-component CCI and intra-component CCI. OP $\mathcal{P}_{\rm out}$ is defined as the probability that the instantaneous end-to-end SINR falls below a threshold $\Theta_{\rm th}$, i.e.,

$$\mathcal{P}_{\rm out} = F_\gamma(\Theta_{\rm th}) = \Pr\left(\frac{\bar{\gamma}_{\rm b}|h_{\rm bd}|^2}{\tilde{I}_{\rm a}+\tilde{I}_{\rm s}+1} \le \Theta_{\rm th}\right). \tag{7}$$

By denoting $\tilde{I} = \tilde{I}_{\rm a}+\tilde{I}_{\rm s}$, the cumulative distribution function (CDF) of the SINR, can be re-expressed as

$$F_\gamma(y) = \int_0^\infty F_{\bar{\gamma}_{\rm b}|h_{\rm bd}|^2}(y(x+1))\,f_{\tilde{I}}(x)\,dx \tag{8}$$

where $\bar{\gamma}_{\rm b}|h_{\rm bd}|^2 = \min\left(\bar{\gamma}_{\rm th}|h_{\rm bd}|^2/|h_{\rm bf}|^2, \bar{\gamma}_{\rm m}|h_{\rm bd}|^2\right)$. Thus,

$$\begin{aligned}F_{\bar{\gamma}_{\rm b}|h_{\rm bd}|^2}(x) &= \Pr\left(|h_{\rm bd}|^2 \le \frac{x}{\bar{\gamma}_{\rm m}}, |h_{\rm bf}|^2 \le \frac{\bar{\gamma}_{\rm th}}{\bar{\gamma}_{\rm m}}\right)\\ &\quad+\Pr\left(|h_{\rm bd}|^2 \le \frac{x}{\bar{\gamma}_{\rm m}}, |h_{\rm bf}|^2 > \frac{\bar{\gamma}_{\rm th}}{\bar{\gamma}_{\rm m}}\right)\\ &\quad+\Pr\left(|h_{\rm bd}|^2 \ge \frac{x}{\bar{\gamma}_{\rm m}}, |h_{\rm bd}|^2 \le \frac{|h_{\rm bf}|^2x}{\bar{\gamma}_{\rm th}}\right) =\\ &\Pr\left(|h_{\rm bd}|^2 \le \frac{x}{\bar{\gamma}_{\rm m}}\right)+\Pr\left(\frac{x}{\bar{\gamma}_{\rm m}} \le |h_{\rm bd}|^2 \le \frac{|h_{\rm bf}|^2x}{\bar{\gamma}_{\rm th}}\right) =\end{aligned}$$

$$F_{|h_{\rm bd}|^2}\left(\frac{x}{\bar{\gamma}_{\rm m}}\right)+\underbrace{\int_{\frac{x}{\bar{\gamma}_{\rm m}}}^\infty f_{|h_{\rm bd}|^2}(y)\int_{\frac{y\bar{\gamma}_{\rm th}}{x}}^\infty f_{|h_{\rm bf}|^2}(z)dzdy}_{\mathcal{J}}. \tag{9}$$

From (5), we can get

$$F_{|h_{\rm bd}|^2}(x/\bar{\gamma}_{\rm m}) = \frac{\Upsilon(k_{\rm bd}, x/(\eta_{\rm bd}\bar{\gamma}_{\rm m}))}{\Gamma(k_{\rm bd})} \tag{10}$$

where $\Upsilon(\cdot,\cdot)$ denotes the lower incomplete Gamma function [11, Eq. (8.350.1)]. Then, the integral $\mathcal{J}$ can be derived as

$$\begin{aligned}\mathcal{J} &= \int_{\frac{x}{\bar{\gamma}_{\rm m}}}^\infty \frac{y^{k_{\rm bd}-1}e^{-\frac{y}{\eta_{\rm bd}}}}{\Gamma(k_{\rm bd})\,\eta_{\rm bd}^{k_{\rm bd}}}\int_{\frac{\bar{\gamma}_{\rm th}y}{x}}^\infty \frac{z^{k_{\rm bf}-1}e^{-\frac{z}{\eta_{\rm bf}}}}{\Gamma(k_{\rm bf})\,\eta_{\rm bf}^{k_{\rm bf}}}dzdy\\ &\overset{\rm (a)}{=} \int_{\frac{x}{\bar{\gamma}_{\rm m}}}^\infty \frac{y^{k_{\rm bd}-1}e^{-\frac{y}{\eta_{\rm bd}}}}{\Gamma(k_{\rm bd})\,\Gamma(k_{\rm bf})\,\eta_{\rm bd}^{k_{\rm bd}}}\Gamma\left(k_{\rm bf}, \frac{\bar{\gamma}_{\rm th}y}{\eta_{\rm bf}x}\right)dy\\ &\overset{\rm (b)}{=} \sum_{m=0}^{k_{\rm bf}-1}\frac{\left(\frac{\bar{\gamma}_{\rm th}}{\eta_{\rm bf}}\right)^m x^{k_{\rm bd}}}{\Gamma(k_{\rm bd})\,\eta_{\rm bd}^{k_{\rm bd}}}\left(\frac{\bar{\gamma}_{\rm th}}{\eta_{\rm bf}}+\frac{x}{\eta_{\rm bd}}\right)^{-\tilde{m}}\Gamma\left(\tilde{m}, \frac{\bar{\gamma}_{\rm th}}{\eta_{\rm bf}\bar{\gamma}_{\rm m}}+\frac{x}{\eta_{\rm bd}\bar{\gamma}_{\rm m}}\right)\end{aligned} \tag{11}$$

where $\tilde{m} = m+k_{\rm bd}$. Here, (a) is obtained with the aid of [11, Eq. (3.351.3)]. In addition, (b) arises by expanding the upper incomplete Gamma function $\Gamma(\cdot,\cdot)$ as [11, Eq. (8.352.2)]. By summing up (10) and (11), $F_{\bar{\gamma}_{\rm b}|h_{\rm bd}|^2}(x)$ can be obtained.

Then, the PDF of $\tilde{I}$ can be written as

$$f_{\tilde{I}}(y) = \mathcal{A}y^{\tilde{l}}e^{-\frac{y}{\tilde{\eta}_{\rm a}}}G_{12}^{11}\left[Qy\,\middle|\,\begin{matrix}-l\\0,-\tilde{l}\end{matrix}\right] \tag{12}$$

where $\mathcal{A} = \sum_{l=0}^{m_{\rm sd}-1}\frac{\alpha_{\rm sd}(-1)^l(1-m_{\rm sd})_l\delta_{\rm sd}^l}{\tilde{\eta}_{\rm a}^{k_{\rm a}}(l!)^2\bar{\gamma}_{\rm s}^{l+1}}$ and $\tilde{l} = l+k_{\rm a}$. The derivation of (12) can be found in Appendix A.

In the integrated network, when the interference dominates the noise, we can approximate $F_\gamma(y)$ as $F_\gamma(y) = \int_0^\infty F_{\bar{\gamma}_{\rm b}|h_{\rm bd}|^2}(xy)\,f_{\tilde{I}}(x)\,dx$. Then, by substituting (10), (11), and (12) into this equation, $F_\gamma(y)$ can be expressed as

$$\begin{aligned}F_\gamma(y) &= \int_0^\infty \frac{\mathcal{A}\Upsilon\left(k_{\rm bd}, \frac{xy}{\eta_{\rm bd}\bar{\gamma}_{\rm m}}\right)}{\Gamma(k_{\rm bd})}x^{\tilde{l}}e^{-\frac{x}{\tilde{\eta}_{\rm a}}}G_{12}^{11}\left[Qx\,\middle|\,\begin{matrix}-l\\0,-\tilde{l}\end{matrix}\right]dx\\ &\quad+\sum_{m=0}^{k_{\rm bf}-1}\frac{\mathcal{A}\left(\frac{\bar{\gamma}_{\rm th}}{\eta_{\rm bf}}\right)^m y^{k_{\rm bd}}}{\Gamma(k_{\rm bd})\,\eta_{\rm bd}^{k_{\rm bd}}}\int_0^\infty x^{\tilde{l}+k_{\rm bd}}\left(\frac{\bar{\gamma}_{\rm th}}{\eta_{\rm bf}}+\frac{xy}{\eta_{\rm bd}}\right)^{-\tilde{m}}\\ &\quad\times\Gamma\left(\tilde{m}, \frac{\bar{\gamma}_{\rm th}}{\eta_{\rm bf}\bar{\gamma}_{\rm m}}+\frac{xy}{\eta_{\rm bd}\bar{\gamma}_{\rm m}}\right)e^{-\frac{x}{\tilde{\eta}_{\rm a}}}G_{12}^{11}\left[Qx\,\middle|\,\begin{matrix}-l\\0,-\tilde{l}\end{matrix}\right]dx.\end{aligned} \tag{13}$$

We define Ψ_1 and Ψ_2 to represent the first integral and the second integral in (13), respectively. The derivations of Ψ_1 and Ψ_2 are given in Appendix B. Finally, by substituting (22), (23), and (25) into (13), the analytical expression for $\mathcal{P}_{\rm out}$ can be obtained as shown in (14), as shown at top of this page.

Special case: To illustrate the CCI in the integrated network intuitively, we focus on analyzing the effect of the interference power constraints imposed by the satellite communication in this part. Specifically, when the satellite receiver is very sensitive ($I_{\rm th}$ is small) or the serving BS is close to the satellite receiver, the transmit power of the serving BS will decrease and mainly be restricted by the interference power

$$\mathcal{P}_{\text{out}} = \mathcal{A}\tilde{\eta}_{\text{a}}^{\tilde{l}+1} G_{22}^{12}\left[Q\tilde{\eta}_{\text{I}} \middle| \begin{matrix} -\tilde{l}, -l \\ 0, -\tilde{l} \end{matrix} \right] - \sum_{i=0}^{k_{\text{bd}}-1} \sum_{j=0}^{L} \frac{\mathcal{A}\left(\frac{\eta_{\text{bd}}\bar{\gamma}_{\text{m}}}{\Theta_{\text{th}}}\right)^{\tilde{l}+j-i+1}}{(-1)^j i! j! \tilde{\eta}_{\text{a}}^{j}} G_{22}^{11}\left[\frac{Q\eta_{\text{bd}}\bar{\gamma}_{\text{m}}}{\Theta_{\text{th}}} \middle| \begin{matrix} -\tilde{l}-j, -l \\ 0, -\tilde{l} \end{matrix} \right] + \sum_{m=0}^{k_{\text{bf}}-1} \frac{\mathcal{A}\Gamma(\tilde{m})}{\Gamma(k_{\text{bd}})\eta_{\text{bd}}^{k_{\text{bd}}}} \times$$
$$\sum_{q=0}^{\tilde{m}-1} \frac{e^{-\frac{\bar{\gamma}_{\text{th}}}{\eta_{\text{bf}}\bar{\gamma}_{\text{m}}}} \left(\frac{\bar{\gamma}_{\text{th}}}{\eta_{\text{bf}}}\right)^{q-k_{\text{bd}}}}{q!\Gamma(\tilde{m}-q)\bar{\gamma}_{\text{m}}^{q}} \sum_{p=0}^{L} \frac{(-1)^p \Theta_{\text{th}}^{k_{\text{bd}}}}{p! Q^{\tilde{l}+k_{\text{bd}}+p+1}} \left(\frac{1}{\tilde{\eta}_{\text{a}}} + \frac{\Theta_{\text{th}}}{\eta_{\text{bd}}\bar{\gamma}_{\text{m}}}\right)^{p} G_{32}^{22}\left[\frac{\eta_{\text{bf}}\Theta_{\text{th}}}{Q\eta_{\text{bd}}\bar{\gamma}_{\text{th}}} \middle| \begin{matrix} -\tilde{l}-k_{\text{bd}}-p, 1-\tilde{m}+q, p-k_{\text{bd}} \\ -k_{\text{a}}-k_{\text{bd}}-p, 0 \end{matrix} \right]. \quad (14)$$

constraints, i.e., $P_{\text{b}} = I_{\text{th}}/|h_{\text{bf}}|^2$. Moreover, we assume h_{bd} undergoes Rayleigh fading, which corresponds to the worst case in Nakagami-m fading. Consequently, the SINR can be expressed as $\gamma = \frac{X}{|h_{\text{bf}}|^2}$ with $X = \frac{\bar{\gamma}_{\text{th}}|h_{\text{bd}}|^2}{\tilde{I}_{\text{a}}+\tilde{I}_{\text{s}}}$. Then, we have $F_{\gamma}(x) = \int_0^{\infty} F_X(xy) f_{|h_{\text{bf}}|^2}(y) dy$. Here, $F_X(x)$ can be given as

$$F_X(x) = \int_0^{\infty}\int_0^{\infty} F_{|h_{\text{bd}}|^2}\left(\frac{x(z+y)}{\bar{\gamma}_{\text{th}}}\right) f_{\tilde{I}_{\text{a}}}(z) f_{\tilde{I}_{\text{s}}}(y) dz dy$$
$$= 1 - M_{\tilde{I}_{\text{a}}}\left(\frac{x}{\bar{\gamma}_{\text{th}}}\right) M_{\tilde{I}_{\text{s}}}\left(\frac{x}{\bar{\gamma}_{\text{th}}}\right) \quad (15)$$

where $M_{\gamma}(\cdot)$ is the moment generating function MGF of the corresponding SINR. From the distribution of the terrestrial aggregate interference and satellite interference presented in Section II, we obtain $M_{\tilde{I}_{\text{a}}}(s) = (1+\tilde{\eta}_{\text{a}}s)^{-k_{\text{a}}}$ and $M_{\tilde{I}_{\text{s}}}(s) = \left(s+\frac{\beta_{\text{sd}}}{\bar{\gamma}_{\text{s}}}\right)^{-1} F\left(m_{\text{sd}}, 1; 1; \frac{\delta_{\text{sd}}}{\bar{\gamma}_{\text{s}}}\left(s+\frac{\beta_{\text{sd}}}{\bar{\gamma}_{\text{s}}}\right)^{-1}\right)$. Applying [11, Eq. (9.121.1)], $M_{\tilde{I}_{\text{s}}}(s)$ can be simplified as $M_{\tilde{I}_{\text{s}}}(s) = \left(s+\frac{\beta_{\text{sd}}}{\bar{\gamma}_{\text{s}}}\right)^{m_{\text{sd}}-1}\left(s+\frac{\beta_{\text{sd}}}{\bar{\gamma}_{\text{s}}}-\frac{\delta_{\text{sd}}}{\bar{\gamma}_{\text{s}}}\right)^{-m_{\text{sd}}}$. As a result, $F_X(x)$ can be derived as

$$F_X(x) = 1 - \sum_{l=0}^{m_{\text{sd}}-1} \frac{C_{m_{\text{sd}}-1}^{l} \beta_{\text{sd}}^{m_{\text{sd}}-l-1} \bar{\gamma}_{\text{s}}^{l+1}}{(\beta_{\text{sd}}-\delta_{\text{sd}})^{m_{\text{sd}}} \bar{\gamma}_{\text{th}}^{l}} x^l \left(1+\frac{\tilde{\eta}_{\text{a}}x}{\bar{\gamma}_{\text{th}}}\right)^{-k_{\text{a}}}$$
$$\times \left(1+\frac{\bar{\gamma}_{\text{s}}x}{(\beta_{\text{sd}}-\delta_{\text{sd}})\bar{\gamma}_{\text{th}}}\right)^{-m_{\text{sd}}}. \quad (16)$$

Then, $F_{\gamma}(x)$ can be expressed as

$$F_{\gamma}(x) = 1 - \sum_{l=0}^{m_{\text{sd}}-1} \frac{C_{m_{\text{sd}}-1}^{l} \beta_{\text{sd}}^{m_{\text{sd}}-l-1} \bar{\gamma}_{\text{s}}^{l+1} x^l}{\Gamma(k_{\text{bf}}) \eta_{\text{bf}}^{k_{\text{bf}}} (\beta_{\text{sd}}-\delta_{\text{sd}})^{m_{\text{sd}}} \bar{\gamma}_{\text{th}}^{l}} \times$$
$$\int_0^{\infty} y^{\tilde{k}_{\text{bf}}} e^{-\frac{y}{\eta_{\text{bf}}}} \left(1+\frac{\tilde{\eta}_{\text{a}}xy}{\bar{\gamma}_{\text{th}}}\right)^{-k_{\text{a}}} \left(1+\frac{\bar{\gamma}_{\text{s}}xy}{(\beta_{\text{sd}}-\delta_{\text{sd}})\bar{\gamma}_{\text{th}}}\right)^{-m_{\text{sd}}} dy \quad (17)$$

where $\tilde{k}_{\text{bf}} = k_{\text{bf}} + l - 1$. By expanding $e^{-\frac{y}{\eta_{\text{bf}}}}$ into series with L terms, expressing polynomials into Meijer-j function with [13, Eq. (10)], and utilizing [11, Eq. (7.811.1)], the OP of the special case, $\tilde{\mathcal{P}}_{\text{out}}$, can be finally obtained as

$$\tilde{\mathcal{P}}_{\text{out}} =$$
$$1 - \sum_{l=0}^{m_{\text{sd}}-1} \sum_{t=0}^{L} \frac{C_{m_{\text{sd}}-1}^{l} \beta_{\text{sd}}^{m_{\text{sd}}-l-1} \bar{\gamma}_{\text{s}}^{l+1} (-1)^t \tilde{\eta}_{\text{a}}^{-l}}{\Gamma(k_{\text{a}})\Gamma(m_{\text{sd}})\Gamma(k_{\text{bf}}) t! (\beta_{\text{sd}}-\delta_{\text{sd}})^{m_{\text{sd}}}}$$
$$\times \left(\frac{\bar{\gamma}_{\text{th}}}{\tilde{\eta}_{\text{a}}\eta_{\text{bf}}\Theta_{\text{th}}}\right)^{k_{\text{bf}}+t} G_{22}^{22}\left[\frac{\bar{\gamma}_{\text{s}}}{(\beta_{\text{sd}}-\delta_{\text{sd}})\tilde{\eta}_{\text{a}}} \middle| \begin{matrix} -\tilde{k}_{\text{bf}}-t, 1-m_{\text{sd}} \\ -\tilde{k}_{\text{bf}}-1-t+k_{\text{a}}, 0 \end{matrix} \right]. \quad (18)$$

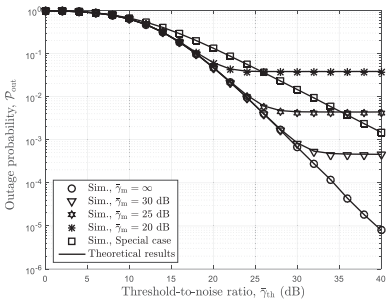

Fig. 1. OP versus $\bar{\gamma}_{\text{th}}$ with various maximum transmit power-to-noise ratios.

IV. Results and Analysis

In this section, numerical simulations were conducted to corroborate our theoretical results and characterize the effects of key parameters on the OP performance. In the simulations, we set $R = 10$ Km and $\Theta_{\text{th}} = 3$ dB. We assume that the satellite interfering link experiences average shadowing with $(m_{\text{sd}}, b_{\text{sd}}, \Omega_{\text{sd}}) = (8, 0.0129, 0.372)$ [8]. For terrestrial links, we set $k_{\Delta} = 2$ and $\eta_{\Delta} = 0.5$.

Fig. 1 illustrates the OP versus interference power threshold-to-noise ratio $\bar{\gamma}_{\text{th}}$ with various maximum transmit power-to-noise ratios $\bar{\gamma}_{\text{m}}$. As observed, the OP under a maximum-power constraint is inferior compared to that of the system with no maximum-power constraint (i.e., $\bar{\gamma}_{\text{m}} = \infty$). Meanwhile, the looser the constraint is, i.e., $\bar{\gamma}_{\text{m}}$ gets larger, the better the OP performance is. It can also be seen that due to the existence of maximum-power constraints, the OP of the cellular user becomes saturated eventually. Moreover, for the special case where the transmit power is only restricted by interference power constraint and the communication link undergoes Rayleigh fading, the OP decreases monotonously when $\bar{\gamma}_{\text{th}}$ increases. In this case, when the interference power constraint is tight, the destination user will suffer from a particularly poor performance for the protection of the satellite receiver. To guarantee the performance of both satellite and terrestrial networks, we should set an exclusion region for the satellite receiver, within which BSs should conduct effective spectrum detection and access to the spectrum holes. Furthermore, we can observe that the theoretical results obtained by (14) and (18) with $L = 30$ agree well with simulations, confirming the accuracy of our derivations and simulations.

Fig. 2 depicts the OP for various interfering configurations, illustrating the impact of two kinds of interference. For terrestrial interference, it can be observed that the OP performance degrades when either the adjacent BS transmit power-to-noise ratio $\bar{\gamma}_{\text{t}}$ increases, or the path loss exponent α decreases, or the intensity of PPP λ increases. For satellite interference, as $\bar{\gamma}_{\text{s}}$ increases, the OP performance degrades when $\bar{\gamma}_{\text{t}}$ is small while

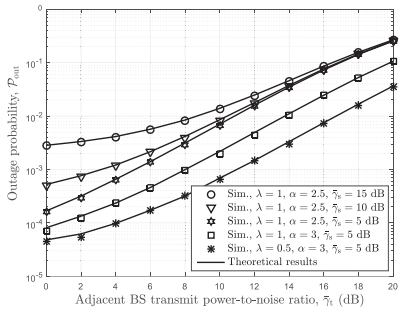

Fig. 2. OP versus $\bar{\gamma}_{\text{t}}$ in various interfering scenarios.

coincides together eventually. The reason for this phenomenon is that as $\bar{\gamma}_{\text{t}}$ increases, interference from adjacent BSs will dominate the total interference received at the destination user.

V. Conclusions

Considering the interference power constraints of satellite communications, we have investigated the OP of an integrated satellite-terrestrial network suffering from hybrid CCI. Simulation results have shown that the performance of the terrestrial communication may be sacrificed when guaranteeing the performance of the satellite communication, which indicates that we should take the requirements of both networks into account when performing frequency reuse.

Appendix A

The PDF of the sum of two independent and non-identically distributed interference, $f_{\tilde{I}}(y)$, can be calculated as

$$f_{\tilde{I}}(y) = \int_0^y f_{\tilde{I}_{\text{s}}}(x)\, f_{\tilde{I}_{\text{a}}}(y-x)\, dx = \frac{\alpha_1}{\bar{\gamma}_{\text{s}}\Gamma(k_{\text{a}})(\tilde{\eta}_{\text{a}})^{k_{\text{a}}}} \times \int_0^y e^{-\frac{y}{\tilde{\eta}_{\text{a}}}}(y-x)^{k_{\text{a}}-1} e^{-\left(\frac{\beta_{\text{sd}}}{\bar{\gamma}_{\text{s}}}-\frac{1}{\tilde{\eta}_{\text{a}}}\right)x}\, {}_1F_1\left(m_{\text{sd}};1;\frac{\delta_{\text{sd}}}{\bar{\gamma}_{\text{s}}}x\right) dx \quad (19)$$

where $\tilde{\eta}_{\text{a}} = \eta_{\text{a}}/N_0$. From [12], we have ${}_1F_1\left(m_{\text{sd}};1;\frac{\delta_{\text{sd}}}{\bar{\gamma}_{\text{s}}}x\right) = e^{\frac{\delta_{\text{sd}}}{\bar{\gamma}_{\text{s}}}x}\sum_{l=0}^{m_{\text{sd}}-1}\frac{(-1)^l(1-m_{\text{sd}})_l(\delta_{\text{sd}}x)^l}{(l!)^2\bar{\gamma}_{\text{s}}^l}$, then $f_{\tilde{I}}(y)$ can be written as

$$f_{\tilde{I}}(y) = \frac{\alpha_{\text{sd}}e^{-\frac{y}{\tilde{\eta}_{\text{a}}}}}{\Gamma(k_{\text{a}})\tilde{\eta}_{\text{a}}^{k_{\text{a}}}}\sum_{k=0}^{m_{\text{sd}}-1}\frac{(-1)^k(1-m_{\text{sd}})_k\delta_{\text{sd}}^k}{(k!)^2\bar{\gamma}_{\text{s}}^{k+1}} \times \int_0^y x^k(y-x)^{k_{\text{a}}-1}e^{-Qx}dx. \quad (20)$$

Here, $(u)_v = \Gamma(u+v)/\Gamma(u)$ is the Pochhammer symbol and $Q = \frac{\beta_{\text{sd}}}{\bar{\gamma}_{\text{s}}} - \frac{1}{\tilde{\eta}_{\text{a}}} - \frac{\delta_{\text{sd}}}{\bar{\gamma}_{\text{s}}}$. By expressing e^{-Qx} in terms of Meijer-j function [13, Eq. (11)] and utilizing [11, Eq. (7.811.2)], the expression of $f_{\tilde{I}}(y)$ can be obtained as (12).

Appendix B

In the derivation of Ψ_1, we expand $\Upsilon(n,x)$ according to [11, Eq. (8.352.1)] and then obtain

$$\Psi_1 = \underbrace{\int_0^\infty Ax^{\tilde{l}}e^{-\frac{x}{\tilde{\eta}_{\text{a}}}}G_{12}^{11}\left[Qx\,\middle|\,\begin{matrix}-l\\0,-\tilde{l}\end{matrix}\right]dx}_{\Xi_1} - \sum_{i=0}^{k_{\text{bd}}-1}\frac{Ay^i}{i!(\eta_{\text{bd}}\bar{\gamma}_{\text{m}})^i} \times \underbrace{\int_0^\infty x^{\tilde{l}}e^{-\frac{x}{\tilde{\eta}_{\text{a}}}}e^{-\frac{xy}{\eta_{\text{bd}}\bar{\gamma}_{\text{m}}}}G_{12}^{11}\left[Qx\,\middle|\,\begin{matrix}-l\\0,-\tilde{l}\end{matrix}\right]dx}_{\Xi_2}. \quad (21)$$

By employing [11, Eq. (7.813.1)], Ξ_1 can be obtained as

$$\Xi_1 = A\tilde{\eta}_{\text{a}}^{\tilde{l}+1}G_{22}^{12}\left[Q\tilde{\eta}_{\text{a}}\,\middle|\,\begin{matrix}-\tilde{l},-l\\0,-\tilde{l}\end{matrix}\right]. \quad (22)$$

In the derivation of Ξ_2, for avoiding the Meijer-j function with two variables, we expand $e^{-\frac{x}{\tilde{\eta}_{\text{a}}}}$ into series with L terms. With the aid of [11, Eq. (7.813.1)], Ξ_2 can be given as

$$\Xi_2 = \sum_{j=0}^{L}\frac{\left(\frac{\eta_{\text{bd}}\bar{\gamma}_{\text{m}}}{y}\right)^{\tilde{l}+j+1}}{(-1)^j j!\tilde{\eta}_{\text{a}}^j}G_{22}^{11}\left[\frac{Q\eta_{\text{bd}}\bar{\gamma}_{\text{m}}}{y}\,\middle|\,\begin{matrix}-\tilde{l}-j,-l\\0,-\tilde{l}\end{matrix}\right]. \quad (23)$$

To obtain Ψ_2, we express $\Gamma(n,x)$ according to [11, Eq. (8.352.2)] and then obtain

$$\Psi_2 = e^{-\frac{\bar{\gamma}_{\text{th}}}{\eta_{\text{bf}}\bar{\gamma}_{\text{m}}}}\sum_{q=0}^{\tilde{m}-1}\frac{\Gamma(\tilde{m})}{q!\bar{\gamma}_{\text{m}}^q}\int_0^\infty x^{\tilde{l}+k_{\text{bd}}}\left(\frac{\bar{\gamma}_{\text{th}}}{\eta_{\text{bf}}}+\frac{xy}{\eta_{\text{bd}}}\right)^{-\tilde{m}+q} \times e^{-\left(\frac{1}{\eta_{\text{I}}}+\frac{y}{\eta_{\text{bd}}\bar{\gamma}_{\text{m}}}\right)x}G_{12}^{11}\left[Qx\,\middle|\,\begin{matrix}-l\\0,-\tilde{l}\end{matrix}\right]dx. \quad (24)$$

Similar to Ξ_2, we expand the exponential term into series with L terms and express $\left(\frac{\bar{\gamma}_{\text{th}}}{\eta_{\text{bf}}}+\frac{xy}{\eta_{\text{bd}}}\right)^{-\tilde{m}+q}$ in terms of Meijer-j function [13, Eq. (10)], Then, applying [11, Eq. (7.811.1)], Ψ_2 can be derived as

$$\Psi_2 = \sum_{q=0}^{\tilde{m}-1}\frac{\Gamma(\tilde{m})e^{-\frac{\bar{\gamma}_{\text{th}}}{\eta_{\text{bf}}\bar{\gamma}_{\text{m}}}}\left(\frac{\bar{\gamma}_{\text{th}}}{\eta_{\text{bf}}}\right)^{q-\tilde{m}}}{\Gamma(\tilde{m}-q)\eta_{\text{bd}}^{k_{\text{bd}}}Q^{\tilde{l}+k_{\text{bd}}+p+1}}\sum_{p=0}^{L}\frac{(-1)^p}{p!q!\bar{\gamma}_{\text{m}}^q}\left(\frac{1}{\tilde{\eta}_{\text{a}}}+\frac{y}{\eta_{\text{bd}}\bar{\gamma}_{\text{m}}}\right)^p \times G_{32}^{22}\left[\frac{\eta_{\text{bf}}y}{Q\eta_{\text{bd}}\bar{\gamma}_{\text{th}}}\,\middle|\,\begin{matrix}-\tilde{l}-k_{\text{bd}}-p,1-\tilde{m}+q,p-k_{\text{bd}}\\-k_{\text{a}}-k_{\text{bd}}-p,0\end{matrix}\right]. \quad (25)$$

References

[1] B. Evans *et al.* "Integration of satellite and terrestrial systems in future multimedia communications," *IEEE Wireless Commun.*, vol. 12, no. 5, pp. 72–80, Oct. 2005.

[2] M. Sadek and S. Aissa, "Personal satellite communication: Technologies and challenges," *IEEE Wireless Commun.*, vol. 19, no. 6, pp. 28–35, Dec. 2012.

[3] V. Deslandes *et al.* "Analysis of interference issues in integrated satellite and terrestrial mobile systems," in *Proc. ASMS/SPSC*, Cagliari, Italy, Sep. 2010, pp. 256–261.

[4] X. Zhu *et al.* "Position-assisted interference coordination for integrated terrestrial-satellite networks," in *Proc. IEEE PIMRC*, Hong Kong, Sep. 2015, pp. 971–975.

[5] K. An *et al.* "Symbol error analysis of hybrid satellite-terrestrial cooperative networks with co-channel interference," *IEEE Commun. Lett.*, vol. 18, no. 11, pp. 1947–1950, Nov. 2014.

[6] G. N. Kamga *et al.* "A unified performance evaluation of integrated mobile satellite systems with ancillary terrestrial component," in *Proc. IEEE ICC*, London, U.K., Jun. 2015, pp. 934–938.

[7] Z. Chen *et al.*, "Aggregate interference modeling in cognitive radio networks with power and contention control," *IEEE Trans. Commun.*, vol. 60, no. 2, pp. 456–468, Feb. 2012.

[8] S. Maleki *et al.*, "Cognitive spectrum utilization in Ka band multibeam satellite communications," *IEEE Commun. Mag.*, vol. 53, no. 3, pp. 24–29, Mar. 2015.

[9] S. Kusaladharma and C. Tellambura, "Aggregate interference analysis for underlay cognitive radio networks," *IEEE Wireless Commun. Lett.*, vol. 1, no. 6, pp. 641–644, Dec. 2012.

[10] A. Abdi *et al.* "A new simple model for land mobile satellite channels: First and second order statistics," *IEEE Trans. Wireless Commun.*, vol. 2, no. 3, pp. 519–528, May 2003.

[11] I. S. Gradshteyn and I. M. Ryzhik, *Table of Integrals, Series, and Products*, 6th ed. Boca Raton, FL, USA: Academic, 2000.

[12] [Online]. Available: http://functions.wolfram.com/07.20.03.0025.01

[13] V. S. Adamchik and O. I. Marichev, "The algorithm for calculating integrals of hypergeometric type functions and its realization in reduce systems," in *Proc. Int. Conf. Symp. Algebraic Comput.*, Tokyo, Japan, 1990, pp. 212–224.